scientific reports

Check for updates

OPEN

Study on incentive mechanism of reward and punishment on work efficiency of PCB welder based on recurrence quantification analysis and electroencephalogram signals

Zhang Qian[1]✉, Mingyue Guo[2] & Fuwang Wang[3]

Traditional methods often struggle to objectively quantify the impact of salary incentives on employees' productivity, leaving enterprise incentive strategies without a solid scientific foundation. To address this issue, this study innovatively combines recurrence quantification analysis (RQA) with electroencephalogram (EEG) signals, proposing a dynamic incentive evaluation model based on the analysis of brain chaos characteristics. By comparing the EEG signals of workers with and without reward and punishment incentives (control group vs. experimental group), key features such as deterministic (DET) and average diagonal line length (DLL) are extracted to reveal how incentives regulate work efficiency. The experiment shows that RQA diagrams of workers' EEG under reward and punishment incentives exhibit significantly enhanced chaotic characteristics, with DET and DLL values decreasing by 13.3% and 10.4%, respectively. The accuracy of the twin support vector machine (TWSVM) reaches 98.71%, which is 0.79% and 14.37% higher than existing EEG-based incentive evaluation methods, such as the phase-locking value combined with convolutional neural network (accuracy: 97.92%) and spectral power features (accuracy: 84.34%). This study not only confirms the feasibility of EEG in incentive evaluation but also addresses the insufficient sensitivity of traditional cognitive load monitoring by integrating RQA features and a dynamic classification framework, providing a quantifiable neuroscientific basis for optimizing enterprise incentive mechanisms.

Keywords Employees' productivity, RQA, EEG signals, Reward and punishment incentives, TWSVM, Accuracy

Measuring the efficiency of printed circuit board (PCB) welding workers under an incentive mechanism of rewards and punishments is of great significance to enterprises. An effective work efficiency assessment not only helps improve production efficiency, ensures product quality, and optimizes the cost structure, but also enhances employee satisfaction, promotes skill improvement, supports decision-making, and ultimately strengthens the competitiveness of enterprises, encourages technological innovation, aligns with corporate social responsibility, and better meets market demand[1]. Therefore, the goal of this study is to objectively assess the efficiency of PCB welding workers under an incentive mechanism of rewards and punishments, providing a basis for enterprises to develop a more scientific and effective incentive system.

In the industrial sector, effectively measuring workers' efficiency under reward and punishment incentives has long been a complex and important issue. Previous studies and practices have proposed various solutions. Oleghe et al. measured worker efficiency using quantitative indicators such as output per unit of time, task completion rate, and accuracy of work performed[2]. Zhou et al. used behavioral observation to evaluate worker efficiency by directly monitoring their behavior during work[3]. VORONKOVA et al. combined self-evaluation and peer evaluation, allowing workers to assess their efficiency while also considering evaluations from colleagues or supervisors[4]. Li et al. employed psychological tests, questionnaires, and other methods to better understand the psychological factors influencing workers' motivation, job satisfaction, and career development needs[5]. However, although these methods can measure work efficiency to some extent, they still have limitations.

[1]School of Economics and Management, Beihua University, Jilin 132013, China. [2]Dongshin University, Jeollanam Do 113-8654, South Korea. [3]School of Mechanic Engineering, Northeast Electric Power University, Jilin 132012, China. ✉email: zhangqian2119909@163.com

Traditional efficiency measurement methods, such as task completion rates, behavioral observation, and self-assessment, have certain drawbacks in accurately assessing productivity. Task completion rate reflects the amount of work completed but does not account for work quality or complexity[6]. Behavioral observation can directly monitor employee activities, but it may lose objectivity due to observer bias or excessive intervention[7]. Self-assessment relies on employees' subjective judgments and is susceptible to personal emotions, cognitive biases, or excessive optimism[8]. These methods fail to fully consider the multi-dimensional nature of work and often struggle to accurately reflect employees' true productivity levels, especially when evaluating complex or creative tasks[9]. In response to these limitations, this study proposes a new measurement method based on employees' electroencephalogram (EEG) signals under different incentive mechanisms, using recursive quantitative analysis to measure welding workers' efficiency, providing a more objective and accurate evaluation method.

EEG signals are the electrical activity of the brain recorded by electrodes placed on the scalp, widely used in the biomedical field, particularly for disease detection[10]. EEG signals can capture neural activity from different brain regions and is commonly used to diagnose neurological diseases such as epilepsy, Parkinson's disease, and sleep disorders[11]. Additionally, EEG signals are employed to evaluate cognitive functions, emotional responses, and stress levels[12]. This paper explores a new application of EEG signals. While EEG has been widely used in neuroscience and clinical diagnosis, its potential in assessing work efficiency has not been sufficiently explored. By analyzing EEG signals, we can identify changes in brain activity across different working states, thereby assessing employees' cognitive load during task execution. This study not only expands the application of EEG beyond the biomedical field but also offers a fresh perspective and scientific basis for optimizing work environments and improving work efficiency. Christie et al. show that reward mechanisms are often associated with positive feedback, pleasant experiences, and motivation in the brain. When a reward-related stimulus is presented, EEG signals display evoked potentials linked to reward anticipation and acquisition, such as P300 waves[13]. Olszewska et al. show that reward incentives are strongly associated with positive emotional experiences, which, in turn, prompt the brain to produce more theta and alpha waves. These brain waves are closely related to relaxation, pleasure, concentration, and positive emotions, especially when completing tasks and receiving rewards. The enhancement of these waves can be seen as a reflection of the brain's "reward response," thus improving attention and work efficiency[14]. In contrast, punishment mechanisms are typically accompanied by negative feedback, stress responses, and negative emotions in the brain[15]. According to Lee et al.'s study, when the punishment mechanism stimulates an individual's stress response, the brain produces more beta waves. An increase in these waves is often linked to tension, anxiety, and excessive focus on the task[16]. Short-term punishment mechanisms can effectively improve alertness and task execution accuracy, particularly in tasks that require error avoidance. Reward and punishment mechanisms produce different EEG signals by regulating distinct neural circuits in the brain, significantly impacting emotions, motivation, and work efficiency. Therefore, this study will analyze EEG signals from employees under both reward and punishment incentive mechanisms, as well as without them, to measure work efficiency. This will provide a theoretical basis for optimizing incentive mechanisms and improving work efficiency.

When using EEG signals to measure the influence of reward and punishment incentives on employee work efficiency, the method of feature extraction is crucial. However, traditional feature extraction techniques have certain limitations. Time-domain feature extraction, the most basic EEG signal analysis method, directly extracts features from the EEG waveform, such as mean, standard deviation, peak value, etc.[17]. However, time-domain features do not capture spectral information and pay less attention to frequency-domain features. Additionally, they are highly sensitive to noise. For frequency-domain feature extraction, the EEG signal is transformed from the time domain to the frequency domain using Fourier transform (FT), allowing for the analysis of the distribution of different frequency components. Common frequency-domain features include power spectral density and band power[18]. However, the traditional FT method struggles to preserve the temporal locality of the signal, making it difficult to capture the instantaneous changes in brain activity. Time–frequency domain analysis methods combine the advantages of both time and frequency domains, enabling simultaneous capture of signal information in both domains. Common time–frequency domain feature extraction methods include wavelet transform (WT) and short-time Fourier transform (STFT)[19]. However, when using STFT, there is a trade-off between time resolution and frequency resolution, and WT faces a similar trade-off in some cases. Additionally, nonlinear analysis methods have become an important direction for EEG signal feature extraction. Common nonlinear methods include fractal dimension, Lyapunov exponent, etc.[20]. While these methods can capture the complexity of EEG signals, they tend to be computationally intensive and lack strong interpretability.

In recent years, deep learning-based EEG classification methods have made significant progress in cognitive load monitoring. For instance, Chakladar et al. used variational autoencoders (VAE) and deep learning models with attention mechanisms to classify cognitive load, achieving classification accuracies of 83.13% and 92.09% for four and two cognitive load states, respectively[21]. Yoo et al. applied long short-term memory networks (LSTM) with attention mechanisms for cognitive load recognition, and their results showed an accuracy rate of 87.1%, outperforming methods like random forests and adaptive boosting[22]. Additionally, researchers have started combining multiple physiological signals, such as heart rate variability (HRV), eye movements, and skin conductance responses, and employing hybrid modeling methods to enhance the accuracy and robustness of cognitive load monitoring. For example, Xiong et al. combined EEG and HRV features and used support vector machines for cognitive load recognition, achieving an accuracy of 97.2%[23]. Studies using multimodal classification methods have shown that physiological markers such as skin conductance response rates, alpha power, alpha peak frequency, and blink rate are closely linked to cognitive load, especially in industrial environments[24]. Recent research on real-time cognitive load monitoring has also progressed significantly. Gutierrez et al. used wearable sensors to collect ECG, EEG, and skin conductance data for real-time workload detection, revealing strong correlations between fatigue features and cognitive load scale scores[25]. Mora-Sanchez et al. developed an eight-channel dry electrode EEG system and proposed an algorithm for real-time cognitive load detection

in classroom environments. Their results demonstrated that theta-band EEG signals could effectively measure cognitive load in classrooms[26]. Although deep learning-based EEG classification methods have shown impressive results in cognitive load monitoring, they still face limitations. For instance, the combination of VAE and deep learning models with attention mechanisms has enhanced classification accuracy, but it remains limited by the diversity and representativeness of the training data and may not fully adapt to various practical scenarios. LSTM and attention mechanisms improve accuracy but are hindered by long training times and high computational resource demands, particularly in real-time applications. Methods that integrate multiple physiological signals (e.g., HRV and skin conductance responses (SCR)) can boost accuracy and robustness, but the complexity of processing multimodal data challenges the models' real-time performance and stability. Furthermore, support vector machines (SVM) combined with multiple physiological signals may be sensitive to noise and have poor adaptability in different environments. To address the limitations of traditional methods, this study proposes the use of the recurrence quantification analysis (RQA) method to analyze the EEG signals of workers under the influence of a reward and punishment incentive mechanism. RQA, developed by Webber et al., specializes in analyzing nonlinear and dynamic systems[27]. It quantifies the recurrent behavior of signals in the phase space, revealing the dynamic structure and complexity of the system, particularly for complex, nonlinear biological signals like those from the brain. RQA also facilitates in-depth analysis of signal behavior at local scales, capturing dynamic changes across different time scales by identifying recurring patterns. Additionally, RQA demonstrates strong robustness, providing reliable dynamic information even when dealing with noisy EEG data. Given these advantages, this study employs RQA to analyze the EEG signals of workers to better understand the effects of reward and punishment incentive mechanisms on brain activity.

This study aims to explore the effect of the reward and punishment incentive mechanism on the work efficiency of welding workers. The RQA method is used to analyze EEG signals to evaluate the work performance of workers under different incentive mechanisms. Firstly, the background and significance of the research are introduced, the limitations of the existing work efficiency evaluation methods are pointed out, and a new evaluation method based on EEG signals is proposed. Then, the experimental design, research methods, and data collection process are described in detail, including subject selection, experimental procedure, EEG signal acquisition, and RQA analysis. The experimental results show that the incentive mechanism significantly improves workers' work efficiency and product quality.

Experiments

Subjects

A total of 30 participants (designated A–J), including 15 males and 15 females with an average age of 30 ± 4.5 years, were recruited for this study. All participants were healthy, with no history of drug use, sleep disorders, or neurological diseases. Prior to the experiment, participants were instructed to avoid alcohol, tea, coffee, and other stimulants to prevent interference with the results. They were also asked to ensure they had adequate sleep before the experiment. All participants provided written informed consent, indicating their voluntary participation and understanding of the study's purpose and procedures. The study protocol was approved by the Ethics Committee of Northeast Electric Power University Hospital and complies with the Declaration of Helsinki and the Ethical Guidelines of the World Medical Association.

Experimental paradigm

In this experiment, participants were required to work for 2 h, performing a PCB soldering task. The experimental design consisted of two rounds. In the first round, participants worked without knowledge of the reward and punishment incentive scheme. In the second round, participants worked after fully understanding the reward and punishment incentive scheme. The second group of subjects had to study the incentive scheme for at least 5 min before the experiment. To ensure the participants did not know the incentive scheme in advance, the experiment was conducted in two stages: first without the incentive mechanism, followed by the experiment with the incentive mechanism. The experiment was scheduled from 2:00 p.m. to 4:05 p.m. During this time, EEG signals were recorded in five separate 5-min sessions. At each session, the experimenter counted the number of solder joints completed by the participants. The specific times for EEG signal acquisition were as follows: the first acquisition was from 2:00 p.m. to 2:05 p.m., the second from 2:30 p.m. to 2:35 p.m., the third from 3:00 p.m. to 3:05 p.m., the fourth from 3:30 p.m. to 3:35 p.m., and the fifth from 4:00 p.m. to 4:05 p.m. After the soldering task, the completed boards were inspected, and the number of faulty solder joints was recorded. The EEG equipment used in this experiment was Emotiv, with a sampling frequency of 128 Hz. The electrode array was arranged according to the international 10–20 system, with 14 channels: AF3, AF4, F3, F4, FC5, FC6, F7, F8, T7, T8, P7, P8, O1, O2. The experimental setup is shown in Fig. 1.

Methods

Incentive mechanism of reward and punishment

A reward and punishment incentive mechanism is a management approach that motivates the behavior and work performance of employees, team members, or organization members through rewards and punishments. Its main purpose is to achieve organizational goals, improve work efficiency, ensure adherence to behavioral norms, and foster the long-term development of the organization through appropriate reward and punishment measures[28]. According to Maslow's hierarchy of needs theory, rewards can fulfill employees' various needs at work, especially their physiological and safety needs. Material rewards, in particular, play a significant role in enhancing employees' motivation[29]. Additionally, Skinner et al. proposed that individual behavior can be shaped through reinforcement and punishment. In the reward and punishment incentive system, positive rewards reinforce desirable behaviors, while negative punishments suppress undesirable ones[30].

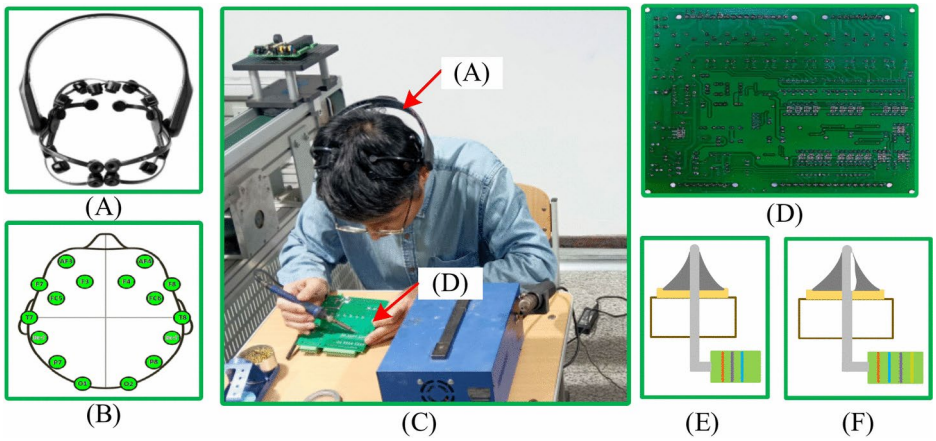

Fig. 1. Experimental scenario. (**A**) Emotiv EEG acquisition device; (**B**) The 10–20 system; (**C**) the subjects participating in the experiment: (**D**) the soldered circuit board in this experiment: (**E**) schematic diagram of qualified solder joints; (**F**) Schematic diagram of solder joint virtual welding.

In recent years, research on reward and punishment has expanded across many fields, including enterprise management, production safety, higher education, and ideological and political education. In enterprise management, a well-designed reward and punishment mechanism can boost employees' enthusiasm and initiative, which in turn improves overall management efficiency[31]. In the field of production, the reward and punishment system is crucial to ensuring safety. By implementing such a system, companies can instill a "sense of responsibility" in every employee, and its formulation and execution are vital for production safety management[32].

The specific content of the incentive mechanism includes the following aspects:

(1) Incentives: Bonuses, salary increases, promotion opportunities, extra vacation or time off, as well as praise and recognition.
(2) Punishment measures: Salary or bonus reductions, reassignment of tasks, changes in position or dismissal, and freezing of promotion opportunities.
(3) Performance evaluation standards: Establish clear performance standards that specify the work objectives employees are expected to achieve. Regular evaluations and feedback should be provided to assess whether the standards for rewards or punishments are met.
(4) Implementation and monitoring of the incentive plan: Monitor the execution of rewards and punishments to ensure fairness and prevent favoritism or bias. Adjust and improve the mechanism based on employee feedback and the actual effectiveness of the incentive system to make it more effective and aligned with employee needs.

In this study, the salary-based reward and penalty system is used to motivate participants. Additionally, EEG signal characteristics are analyzed to examine whether the reward and punishment mechanism causes changes in participants' physiological responses. The objective evaluation criteria for the reward and punishment system are then established to improve employee work efficiency.

RQA method

The recurrence plot (RP) method reflects the behavior of time series in which similar states appear at specific moments. RP analysis was first proposed by Eckmann et al. in 1987 and effectively reveals the dynamic changes of the signal. RP is a two-dimensional matrix composed of 0 s and 1 s, which maps a one-dimensional time series to a high-dimensional phase space and visualizes it in two dimensions, showing the distance between vectors in that space. During the calculation process, an appropriate threshold must be chosen: if the distance between two vectors exceeds this threshold, the matrix value is 1; if the distance is below this threshold, the matrix value is 0. Based on the principle of symbolic dynamics, the order recurrence plot (ORP) improves on traditional RP by symbolizing the sorting of vectors in the high-dimensional phase space, thus reducing errors and computational complexity caused by threshold selection[33]. This study plotted the ORP based on EEG signals under a reward-punishment incentive mechanism and extracted features using the RQA method.

Compared to other methods such as wavelet transform, entropy-based analysis, and fractal dimension methods, RQA has unique advantages in analyzing EEG signals. RQA can effectively capture the nonlinear, dynamical characteristics, and complex behaviors of a system by analyzing the reconstruction of the phase space and the similarity of the signal's trajectories. This method is particularly effective at identifying and quantifying both periodic and aperiodic features, making it suitable for revealing potential patterns in EEG signals. Wavelet transform primarily focuses on frequency domain characteristics, often overlooking the long-term dependencies and complex dynamic behaviors within the time series[34]. The entropy-based method focuses on chaos or uncertainty but does not directly reflect the signal's specific time structure[35]. The fractal dimension method can reveal the signal's self-similarity but lacks the intuitive approach of RQA in handling complex dynamic

changes[36]. Therefore, RQA provides more comprehensive and detailed insights into the nonlinear dynamical behaviors of EEG signals, making it especially useful for studying complex brain activity patterns and signal changes in pathological states.

Phase space reconstruction

Phase space reconstruction (PSR) is a method to extract chaotic behavior information of the system, and the ORP of nonlinear time series reflects its characteristics in high-dimensional phase space. In this study, we used PSR as the basis for analyzing the recurrence properties of EEG signals to construct the ORP and RQA.

Takens proposes the embedding theorem as an efficient solution for PSR. This theorem demonstrates that by selecting appropriate time delays and embedding dimensions, one can reconstruct nonlinear time series into a high-dimensional phase space, preserving their topological properties[37].

Let the time series be $\{(x)|n = 1, 2, \ldots\ldots, N\}$ with length N, embedding dimension m, and delay time τ. After PSR, m-dimensional vectors are obtained, as shown in Eq. (1).

$$X(n) = (x(n), x(n+\tau), \ldots, x(n+(m-1)\tau)), \quad n = 1, 2, \ldots, N-(m-1)\tau \tag{1}$$

According to Eq. (1), the factors that affect the quality of PSR are the embedding dimension m and the delay time τ. An improper selection of delay time τ and embedding dimension m will affect the whole system. If the delay time τ is not selected properly, there will be problems such as phase space trajectory distortion or weak correlations between vectors. When the embedding dimension m is not chosen properly, the high-dimensional space obtained by reconstruction will contain not only the points from the existing space but also points from the original space. At the same time, the larger m is, the more the computational complexity will increase. Therefore, the selection of appropriate phase space parameters plays a decisive role in the subsequent generation of ORP and quantitative analysis.

Existing methods for determining the embedding dimension include geometric invariant analysis and the false nearest neighbor (FNN) algorithm. For delay time, common methods include the autocorrelation coefficient, average displacement, and mutual information (MI) methods. Among these, the FNN and MI algorithms are the most widely used. Therefore, in this study, the FNN algorithm is used to determine the embedding dimension, and the MI algorithm is used to determine the delay time.

Selection of the optimal embedding dimension m When reconstructing the phase space, the motion state in the high dimension is mapped to the low dimension. As the dimension decreases, the non-adjacent points will coincide in the projection process. These points are not adjacent in the original space, so these meaningless neighbours are called false nearest neighbors. As the dimension increases, the trajectory will be slowly restored and the false neighbours will disappear, resulting in the FNN method.

Combined with Eq. (1), assuming $X_m(n)$ phase space m dimensional, there is always a nearest neighbor point $X_m(n\prime)$ of $X_m(n)$:

$$X_m(n') = x(n'), x(n'+\tau), \ldots x[n'+(m-1)\tau] \qquad n' = 1, 2, \ldots, N-(m-1)\tau, n' \neq n \tag{2}$$

The euclidean distance between them is:

$$Y_m(n, n') = \parallel X_m(n), X_m(n') \parallel \tag{3}$$

When m dimension rises to $m+1$ dimension, the Euclidean distance between the two will also change, assuming that it is denoted by $Y_{m+1}(n, n')$, then:

$$Y_{m+1} = \sqrt{[Y_m(n, n')]^2 + [x(n+m\tau) - x(n'+m\tau)]^2} \tag{4}$$

When there is a large difference between them, it means that two non-adjacent points of the trajectory coincide in the process of projection to the lower dimension, which is a false neighbour point.

Introduce the variable: $Q_1(m, m)$

$$Q_1(m, n) = \sqrt{\frac{[x(n+m\tau) - x(n+m\tau)]^2}{[Y_m(n, n')]^2}} \tag{5}$$

If $Q_1(m, n) > Q_\tau$, then $Y_{m+1}(n, n')$ is the false nearest neighbor point and Q_t is the threshold.

Theoretically, when the embedding dimension m is large enough, the number of false neighbours will tend to zero. However, in practical applications, time series are affected by factors such as measurement accuracy and noise, and the number of false neighbouring points is not always 0, and m is too large to model and predict small sample data. Therefore, in the calculation process, starting from the assumed minimum embedding dimension, the value of m is gradually increased. When the proportion of the number of false neighbouring points is less than 5% or their number no longer decreases with the increase of m, the chaotic motion trajectory can be considered to be fully expanded, and the value at this time is the optimal embedding dimension of PSR[38].

The selection of delay time τ MI is a physical concept that is generally used to measure the correlation between two events and is a measure of the interdependence between two random variables[39]. This study employs the MI method to calculate the delay time, utilizing the following algorithm:

Let two systems *S*, *Q* consist of $\{ S_1, S_2, \ldots, S_m \}$ and $\{q_1, q_2, \ldots, q_n\}$, respectively. The information entropy is as follows.

$$H(S) = -\sum_{i=1}^{m} P_S(s_i) \log_2 P_S(s_i) \tag{6}$$

$$H(Q) = -\sum_{j=1}^{n} P_Q(q_j) \log_2 P_Q(q_j) \tag{7}$$

MI is calculated as follows.

$$\mathrm{I(S,\ Q)} = \mathrm{H(S)} + \mathrm{H(Q)} - \mathrm{H(S,\ Q)} \tag{8}$$

$$H(S,Q) = -\sum_{i=1}^{m}\sum_{j=1}^{n} P_{S,Q}(s_i, q_j) \log_2 P_{S,Q}(s_i, q_j) \tag{9}$$

In Eq. (8), MI represents the shared information quantity between the two systems, which is obtained by subtracting the joint entropy H(S,Q) from the sum of their individual entropies. Where $P_S(s_i)$ and $P_Q(q_j)$ are the probabilities of the states of the two systems at time *i* and *j*; $P_{S,Q}(s_i, q_j)$ is the joint distribution probability of both.

MI is normalized to:

$$I_{norm}(S,Q) = \frac{I(S,Q)}{\sqrt{H(S) \times H(Q)}} \tag{10}$$

The EEG signal is introduced to further analyze $S = (x)$, assuming $Q = x(n+\tau)$, then the MI of both is a function with respect to τ.

$$I(\tau) = \frac{I(x(n), x(n+\tau))}{\sqrt{H(x(n)) \times H(x(n+\tau))}} \tag{11}$$

The minimum value of $I(\tau)$ indicates that the nonlinear time series $x(n)$ and $x(n+\tau)$ are maximally possibly uncorrelated, and then the first minimum value of $I(\tau)$ is the optimal time delay τ.

ORP

ORP visualizes time series signals in high-dimensional phase space in two-dimensional space to observe the recursive characteristics of high-dimensional signals[40]. The vectors reconstructed from phase space are symbolized by first taking $m=2$ as an example, and for time series $\{x(n)|x = 1, 2, 3, \ldots, N\}$, the set of reconstructed vectors is $X(n) = (x(n), x(n+\tau))$.

The vector set after phase space reconstruction is symbolized as: π_n, as shown in Eq. (12):

$$\pi_n = \begin{cases} 0, & x(n) < x(n+\tau) \\ 1, & x(n) > x(n+\tau) \end{cases} \tag{12}$$

At this time, according to Eq. (12), it can be seen that the reconstructed vector set has two states: rising and falling.

When the embedding dimension $m=3$, the reconstructed vector set $X(n) = (x(n), x(n+\tau), x(n+2\tau))$ results in six ordering states, as shown in Fig. 2.

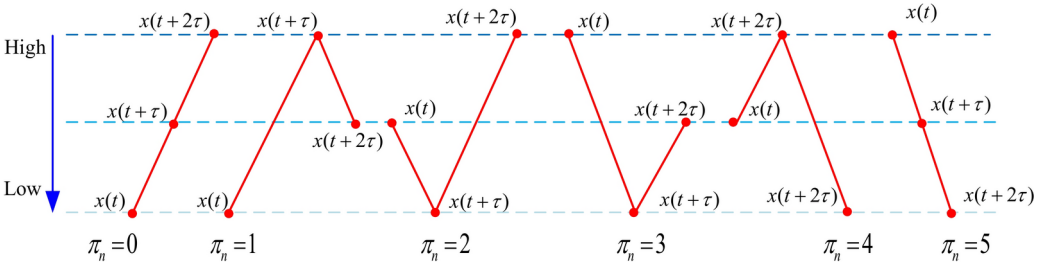

Fig. 2. Six ordering states for the $m=3$ vector set.

Figure 2 shows that when the embedding dimension is m, $m!$ According to the sorting pattern, the sorting state at different times is calculated, and the sorting recurrence matrix is calculated, as shown in Eq. (13) :

$$OR_{ij} = \begin{cases} 0, & \pi_i \neq \pi_j \\ 1, & \pi_i = \pi_j \end{cases} \tag{13}$$

In Eq. (13), when the ordering is the same at two instants, $OR_{ij} = 1$, and blue dots appear on ORP. When the two instants are sorted differently, $OR_{ij} = 0$ and white dots appear on ORP. So ORP is composed of blue and white points generated by 0,1, and the number of rows and columns is $N - (m-1)\tau$. In order to better show the drawing process of ORP, the 10 s EEG signal of subject A is selected, the embedding dimension is chosen as 3, the time delay is τ, and the ORP flow chart is drawn as shown in Fig. 3.

Figure 4 illustrates the ORP plotted for different signal types. Figure 4A shows the ORP plotted by the cosine signal, which is a periodic signal. Figure 4B shows the OPR plotted by the EEG signal of time, which is a chaotic signal. Both are 800 pieces of data.

The cosine signal in Fig. 4A is a periodic signal, and its ORP presents a more clear, neat and ordered texture, reflecting obvious regularity. In contrast, the chaotic signal in Fig. 4B, whose ORP has small white squares and blue squares, shows trivial and disorganized characteristics as a whole, lacking obvious regularity.

RQA method

The ORP diagram intuitively reflects the trend and changes in the signal. However, for aperiodic signals or random sequences, the image often lacks clear regularity, and these changes cannot be easily quantified. To address this, the RQA method is used to quantify the features derived from the ORP map. The parameters involved in RQA in this study include determinacy (DET) and average diagonal line length (DLL). Using DET and DLL to analyze brain activity effectively captures the nonlinear and dynamic characteristics under changes in cognitive load. Cognitive load changes are often accompanied by nonlinear brain activity fluctuations. RQA reveals the complex dynamics of brain signals through DET and DLL. DET reflects the system's determinacy (predictable part), while DLL is related to the system's sensitivity (Lyapunov exponent) and can capture the chaos and complexity of the signal. Therefore, it provides a more accurate description of cognitive load changes than

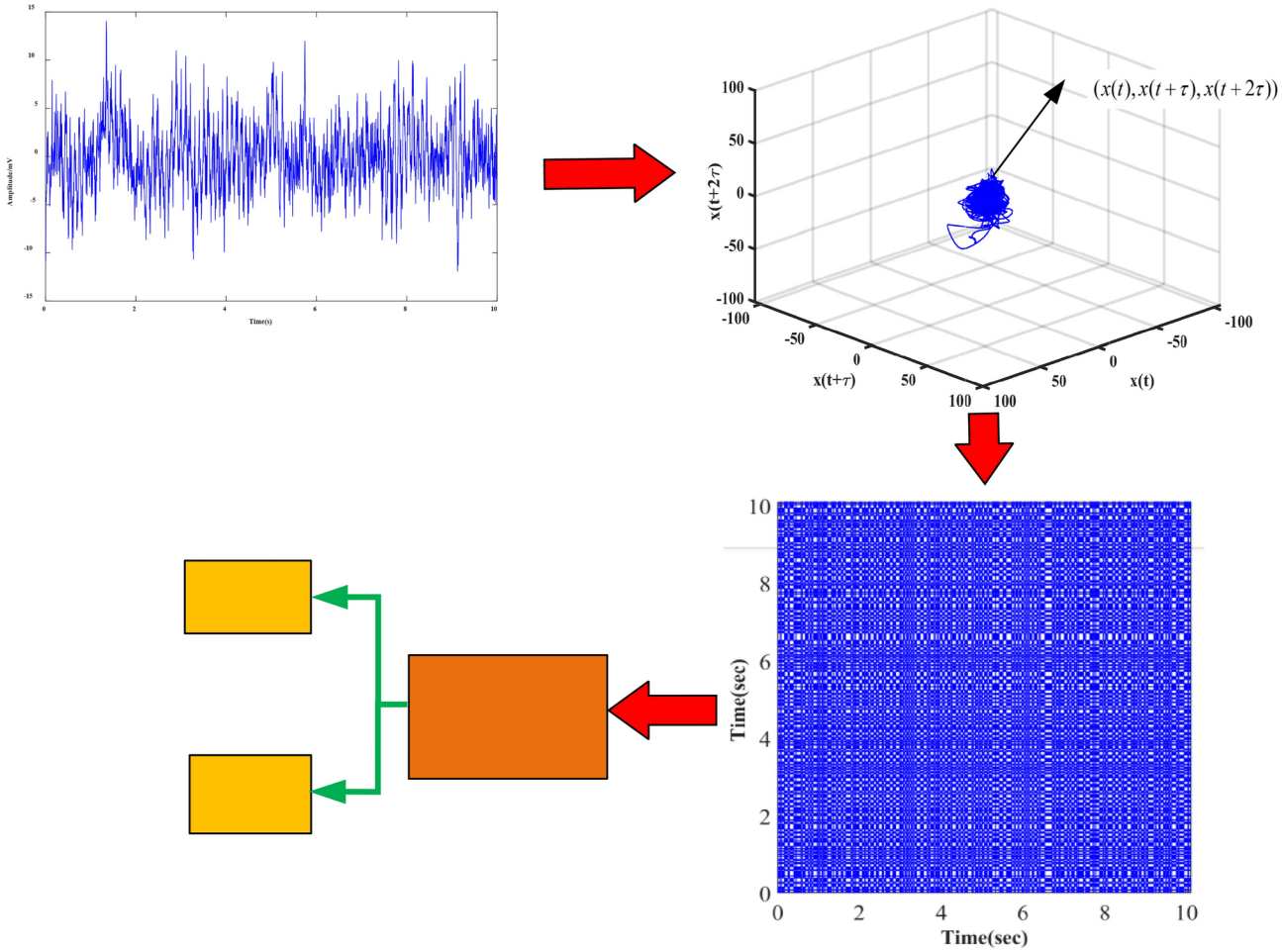

Fig. 3. The process plotted by ORP.

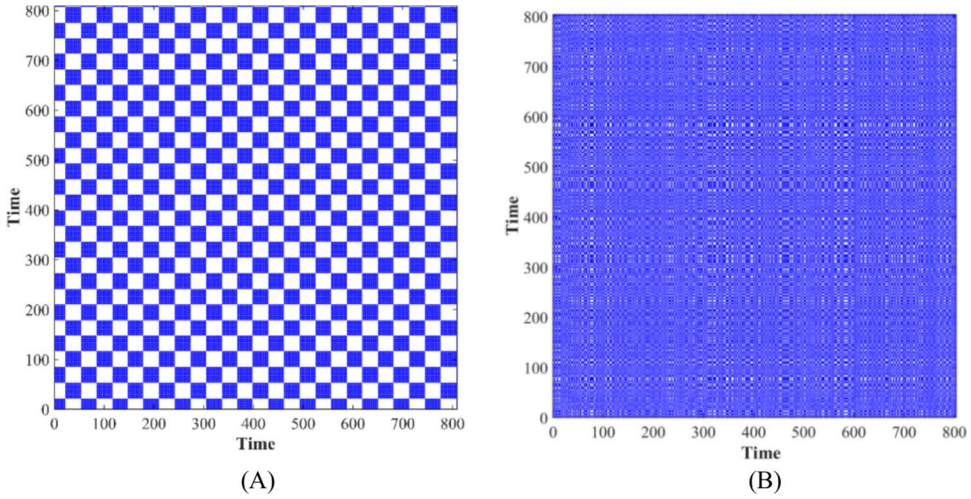

Fig. 4. Plotted ORP for different signal types. (**A**) ORP plotted by cosine signal (periodic signal); (**B**) ORPdrawn from EEG signal of human (chaotic signal) under incentive mechanism of reward and punishment.

traditional methods, such as permutation entropy and the Hurst index. Moreover, RQA captures the time series dependencies in brain activity by reconstructing the phase space of the time series, which reflects the influence of past activities on future performance. In contrast, permutation entropy focuses more on local uncertainty, while the Hurst index emphasizes long-term memory characteristics. However, RQA outperforms these methods in dealing with complex nonlinear and chaotic behaviors. RQA aligns with the theory of complex systems and can reflect the dynamic behavior of the brain as a complex system. Especially under high cognitive load, DET and DLL can quantify nonlinear and chaotic states, while permutation entropy and the Hurst index are more limited. Finally, RQA is more robust in noisy environments and can accurately reflect the system's real dynamic characteristics, while permutation entropy and the Hurst index may be affected by noise, leading to unstable results. Therefore, this study selects DET and DLL as the characteristic parameters. The calculation methods for these parameters and their meanings are described in detail below.

(1) DET refers to the ratio of the number of recurrence points in the line segment parallel to the main diagonal in the ORP diagram to the total number of recurrence points in the diagram, which reflects the proportion of deterministic structures and the recurrence degree of the signal. The specific calculation method is shown in Eq. (14):

$$DET = \frac{\sum_{l=l_{\min}}^{N-1} lP(l)}{\sum_{i,j=1}^{N} R_{i,j}} \tag{14}$$

(2) In Eq. (14), l is the length of the line segment, and $P(l)$ is the probability distribution of the occurrence of the line segment of length l. $l_{\min}$ is the threshold of the length of the line segment, and only if the length of the line segment is greater than this threshold, it will be counted in the statistics.
(3) DLL is the weighted average of the number of recurrence points in the line segments parallel to the main diagonal. The specific calculation method is shown in Eq. (15):

$$DLL = \frac{\sum_{l=l_{ln}}^{N} lP(l)}{\sum_{l=l_{\min}}^{N} P(l)} \tag{15}$$

In Eq. (15), l is the length of the line segment, and $P(l)$ is the probability distribution of the occurrence of the line segment of length l. Similar to DET, DLL reflects the degree of certainty of the system; the larger the DLL, the smaller the randomness of the system. Conversely, the smaller the DLL, the greater the randomness of the system.

Twin support vector machine

As an improved version of conventional SVM, the twin support vector machine (TWSVM) separates positive and negative samples by solving a set of non-parallel hyperplanes. In terms of time complexity, TWSVM operates more efficiently because it transforms the classification problem into two SVM models, making its time cost approximately a quarter of that of conventional SVM. This study chose TWSVM over deep learning models for the following reasons: First, TWSVM performs better in scenarios with small sample sizes. Since the EEG dataset used in this study is relatively small, deep learning models, such as convolutional neural networks (CNN) and LSTM, usually require a larger dataset to avoid overfitting. In contrast, TWSVM, by constructing

dual hyperplanes to optimize the classification boundary, demonstrates stronger generalization ability in small sample environments[41]. Second, TWSVM has high computational efficiency and interpretability. Its linear complexity makes it suitable for real-time processing, such as with embedded EEG devices. Additionally, its decision-making process can be intuitively explained using hyperplane geometry, which is important for the transparency required in clinical or cognitive research[42]. In contrast, the "black box" nature of deep learning models may limit their use in sensitive areas, such as medical diagnostics. Finally, TWSVM exhibits superior robustness to noise. EEG signals are often affected by motion artifacts or environmental interference, and by maximizing the margin, TWSVM naturally handles some noise. In contrast, unregularized CNN models may overfit due to noise interference.

Suppose that the set of training samples in n-dimensional space is $\left(x_j^i, y_j\right), i = 1, 2; j = 1, 2 \cdots t, y_j \in \{1, -1\}$, where x_i^j represents the jth sample belonging to class i and y_j represents the class of the jth sample. Let matrix $A \in R^{t_1 \times n}$ represent the set of samples of the positive class, matrix $B \in R^{t_2 \times n}$ represent the set of samples of the negative class, where t_1 and t_2 represent the number of samples of the positive class and negative class, respectively. The definition is as follows:

(1) Construct two hyperplanes, in which the positive hyperplane A is closer to the positive sample class and away from the negative sample class, and the negative hyperplane B is closer to the negative sample class and away from the positive sample class.
(2) Decompose the solution of the hyperplane into two quadratic programming problems:

$$\begin{aligned} &(\text{TWSVM1}) \min \frac{1}{2}(Aw_1 + eb_1)^T(Aw_1 + eb_1) + c_1 e_2^T \xi \\ &s.t. \ -(Bw_1 + e_2 b_1) + \xi \geq e_2, \xi \geq 0 \\ &(\text{TWSVM2}) \min \frac{1}{2}(Bw_2 + eb_2)^T(Bw_2 + eb_2) + c_2 e_1^T \eta \\ &s.t. -(Aw_2 + e_1 b_2) + \eta \geq e_1, \eta \geq 0 \end{aligned} \tag{16}$$

where $e_1 = (1, \ldots 1)^{\mathrm{T}} \in R^{t_1}; e_2 = (1, \ldots 1)^{\mathrm{T}} \in R^{t_2}$.

(3) Apply the dual transformation to it:

$$\begin{aligned} &(\text{TWSVM1}) \max_{\alpha} e_2^T \alpha - \frac{1}{2}\alpha G(H^T H)^{-1} G^T \alpha \\ &s.t. 0 \leq \alpha \leq c_1 \\ &(\text{TWSVM2}) \max_{\beta} e_1^T \beta - \frac{1}{2}\beta P(Q^T Q)^{-1} P^T \beta \\ &s.t. \ 0 \leq \beta \leq c_2 n \end{aligned} \tag{17}$$

where $H = \begin{bmatrix} A^T & e_1^T \end{bmatrix}, G = \begin{bmatrix} B^T & e_2^T \end{bmatrix}, Q = \begin{bmatrix} B^T & e_2^T \end{bmatrix}, P = \begin{bmatrix} A^T & e_1^T \end{bmatrix}$.

(4) Finally, the classification decision function of TWSVM is obtained as follows.

$$Label(x) = \arg\min_i (c_i) = \arg\min_i |x^T w_i + b_i| = \begin{cases} c_1 \Rightarrow class1 \\ c_2 \Rightarrow class2 \end{cases}, i = 1, 2 \tag{18}$$

Results

During dataset preprocessing and artifact removal, we first eliminated electrooculogram (EOG) and electromyogram (EMG) artifacts using independent component analysis (ICA). Next, we reduced high-frequency noise with the wavelet threshold method. To handle outliers, we applied the RobustScaler method for data standardization, which is based on the median and interquartile range. We used the K-S test to verify the differences among subjects and found $p > 0.05$, indicating no significant difference between them.

Plotting ORP

Since the embedding dimension and delay time after phase space reconstruction have an important impact on the subsequent ORP rendering, the optimal embedding dimension and delay time are first determined in this study.

Calculate the optimal embedding dimension

In this study, the 8-s EEG signal of subject A on channel O1 was selected and the FNN method was used to find the optimal embedding dimension. The curve of the number of false adjacent points as a function of embedding dimension is shown in Fig. 5.

Figure 5 shows that when the embedding dimension is 3, the number of false adjacent points no longer decreases as the value of m increases. Therefore, the optimal embedding dimension for phase space reconstruction of this segment signal is three.

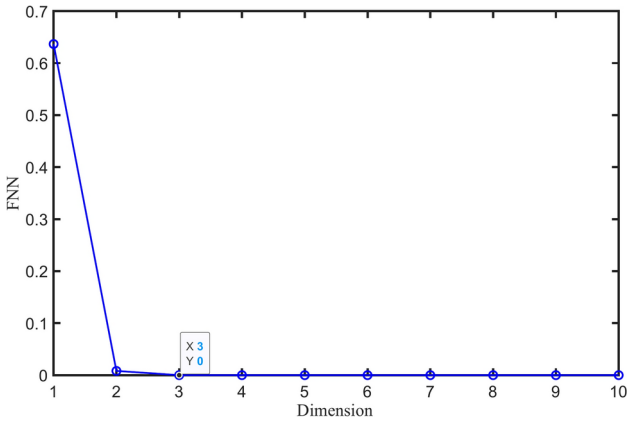

Fig. 5. Curve of the number of false adjacent points as a function of embedding dimension.

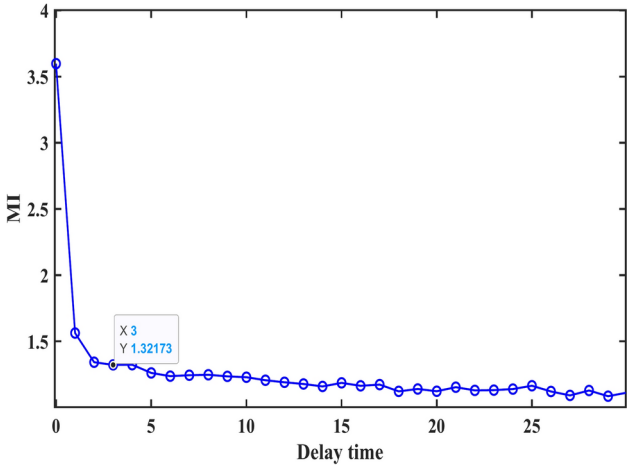

Fig. 6. Curve of MI as a function of delay time τ.

Calculate the optimal delay time

The mutual information I_τ is calculated for different values of delay time τ, and the curve of the relationship between I_τ and delay time τ is drawn. The delay time τ corresponding to the first minimum value of I_τ is taken as the optimal delay time. In this study, an EEG signal of 8 s was selected and the MI method was used to find the optimal delay time, as shown in Fig. 6.

It can be seen from Fig. 6 that I_τ corresponds to the first minimum point when the delay time is 3. Therefore, the optimal delay time for phase space reconstruction of the signal in this segment is 3.

ORP

The study selects channels F3, F4, O1, and O2 because EEG signals from these brain areas can reflect key cognitive activities and the working state of individuals during task execution. By monitoring the activity in these regions in real-time, the work efficiency, attention level, and fatigue of workers can be more accurately evaluated, providing important insights for improving efficiency and reducing fatigue[43]. Previous studies have shown that this selection of channels is effective for this type of research. In this study, the EEG signals from channels F3, F4, O1, and O2 of subject A were analyzed under two working conditions: one with a reward and punishment incentive mechanism, and the other without[44]. The FNN method was used to determine the optimal embedding dimension, and the MI method was employed to find the optimal delay time. The ORP for both conditions was then plotted, with the results shown in Figs. 7, 8, 9, and 10.

In ORP, when the ordering states of the two moments are the same, $OR = 1$, represented by a blue dot on the figure. When the ordering states differ, $OR = 0$, represented by a white dot. This results in a blue-and-white binary matrix diagram of ORP. From Figs. 7, 8, 9, and 10, we can observe a clear difference in the ORP plotted for the EEG signals of four channels (F3, F4, O1, and O2) between the two working states. Under the condition without a reward or punishment incentive mechanism, the white and blue squares in the ORP are larger, more regularly arranged, and clearer in texture, indicating weak chaos in the EEG signals. In contrast, under the condition with a reward and punishment incentive mechanism, the white and blue squares in the ORP are smaller and more randomly arranged, suggesting stronger chaos in the EEG signals.

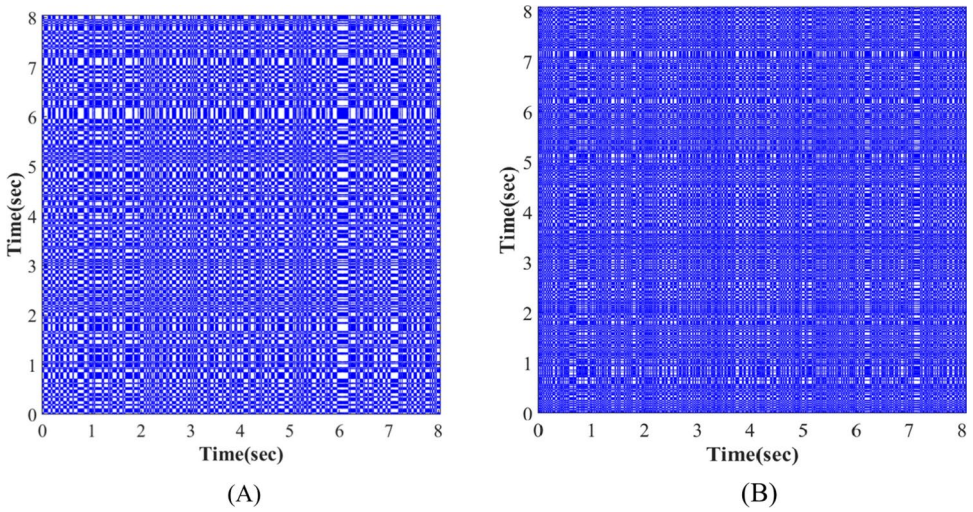

Fig. 7. ORP of EEG signals from the F3 channel in two working states. (**A**) No reward and punishment incentive mechanism; (**B**) Reward and punishment incentive mechanism.

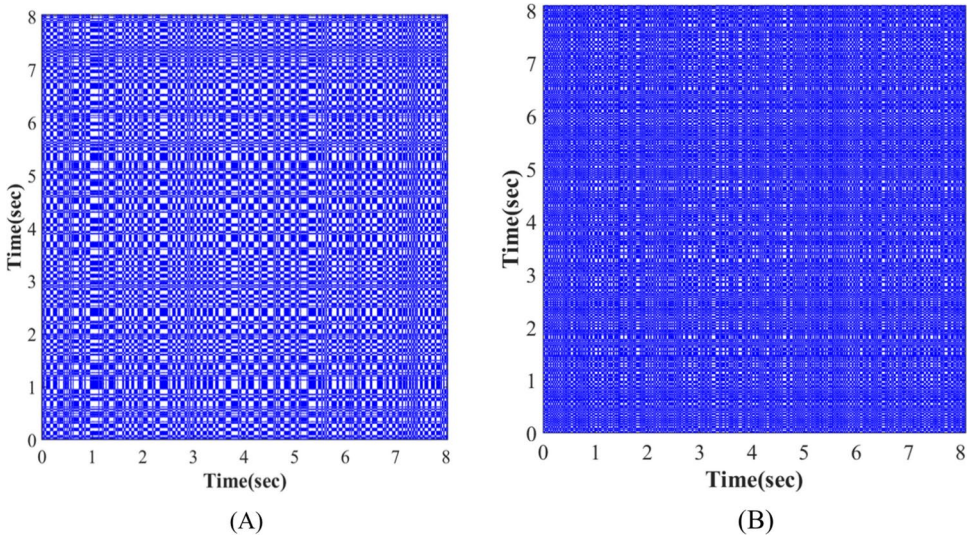

Fig. 8. ORP of EEG signals from the F4 channel in two working states. (**A**) No reward and punishment incentive mechanism; (**B**) Reward and punishment incentive mechanism.

RQA

In this study, the RQA method was used to perform ORP analysis on the EEG signals of subject A on four EEG channels (F3, F4, O1, O2), and the quantization parameters DET and DLL were calculated in the two working states. The result is shown in Fig. 11.

Figure 11 shows that under the two working conditions, there are significant differences in the DET and DLL values of the ORP derived from EEG signals of the four EEG channels. The DET and DLL values under the reward and punishment incentive mechanism are lower than those without the incentive mechanism. A t-test was performed on the data in Fig. 11, revealing that the p-value for DET was 0.045 (less than 0.05), and the p-value for DLL was 0.0002 (also less than 0.05). Therefore, there was a significant difference between the two groups. The reward and punishment incentive mechanism proposed in this study can effectively enhance workers' work efficiency.

Additionally, the ORP of the four EEG channels from 10 subjects was analyzed using RQA, and the results are shown in Fig. 12.

Figure 12 shows that the DET and DLL values of the 10 subjects in the four EEG channels were lower under the reward and punishment incentive mechanism than under the no reward and punishment incentive mechanism. This suggests that the reward and punishment incentive mechanism reduces the certainty of the EEG signal and increases its randomness. A t-test was performed on the data in Fig. 12, which revealed that the p-value for DET was 0.045 (less than 0.05), and the p-value for DLL was 0.0002 (also less than 0.05).

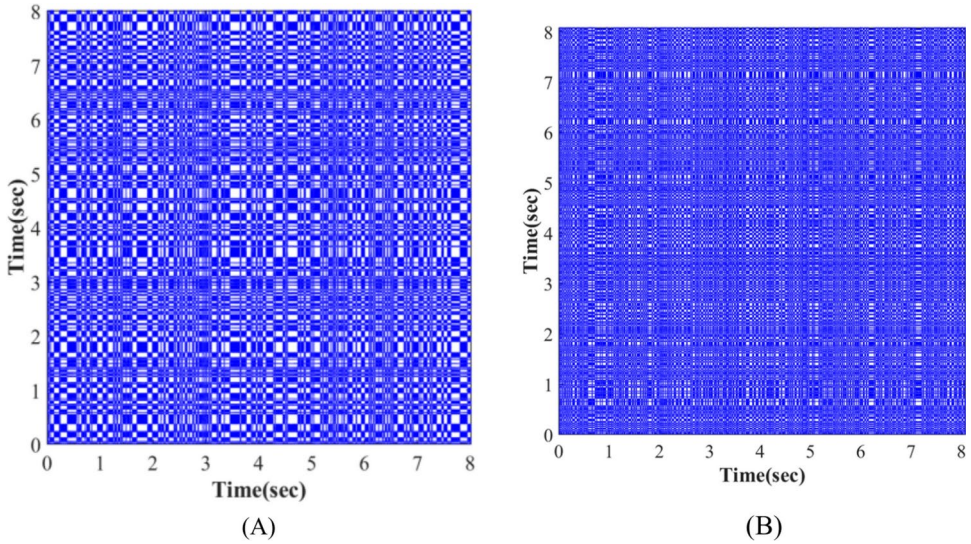

Fig. 9. ORP of EEG signals from the O1 channel in two working states. (**A**) No reward and punishment incentive mechanism; (**B**) Reward and punishment incentive mechanism.

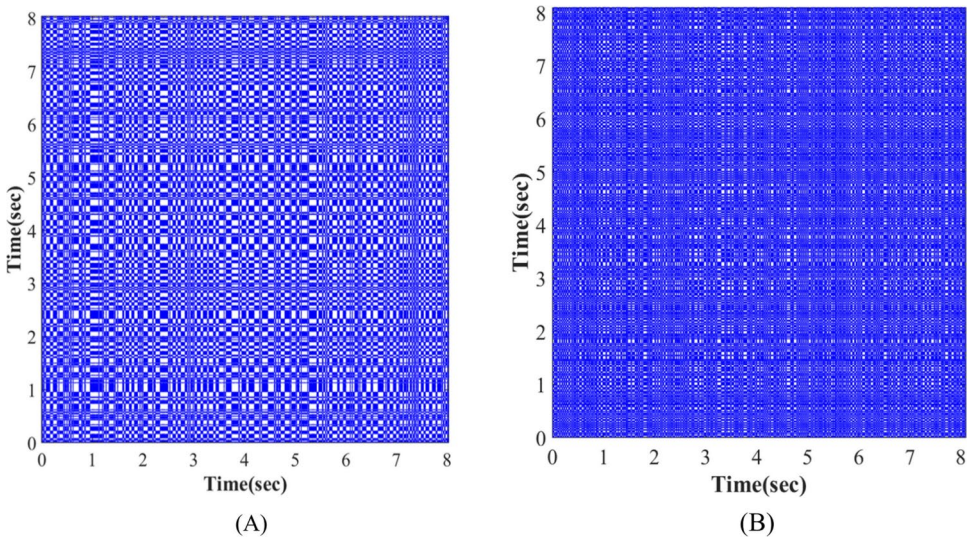

Fig. 10. ORP of EEG signals from the O2 channel in two working states. (**A**) No reward and punishment incentive mechanism; (**B**) Reward and punishment incentive mechanism.

Classification results

In this study, the RQA method was used to analyze EEG signals and extract two features: DET and DLL. Based on these features, a feature matrix was constructed and input into TWSVM for binary classification. In the feature matrix, each row represents a sample (data point), and each column represents a feature (attribute or variable). The feature matrix constructed in this study is a two-dimensional matrix with 500 samples and 2 features, resulting in a matrix size of 500×2. The data in the feature matrix are numerical. To improve the performance of the TWSVM model, the feature matrix was standardized. The computer used in the experiment was configured with a 13th-generation Core i9-13900HX high-performance processor, an RTX 4060 dedicated graphics card, and 16 GB of RAM. The TWSVM algorithm was implemented in the R programming environment and executed in Matlab 2022b software. Furthermore, wavelet entropy and machine learning methods were combined to analyze EEG signals under different excitation mechanisms. The wavelet entropy features for each excitation mechanism were extracted, and the feature matrix was constructed and input into the TWSVM method for classification. The classification results of 10 subjects are shown in Table 1.

Table 1 compares the performance of the RQA method with other advanced methods in terms of accuracy, precision, recall, and F1 score. Among these, the accuracy of the DET value is 97.64%, the precision is 97.29%, the recall is 96.96%, and the F1 score is 97.14%. The accuracy of the DLL value is the highest, reaching 98.71%, with a precision of 97.54%, a recall of 98.29%, and an F1 score of 97.91%. Among other methods, the combination

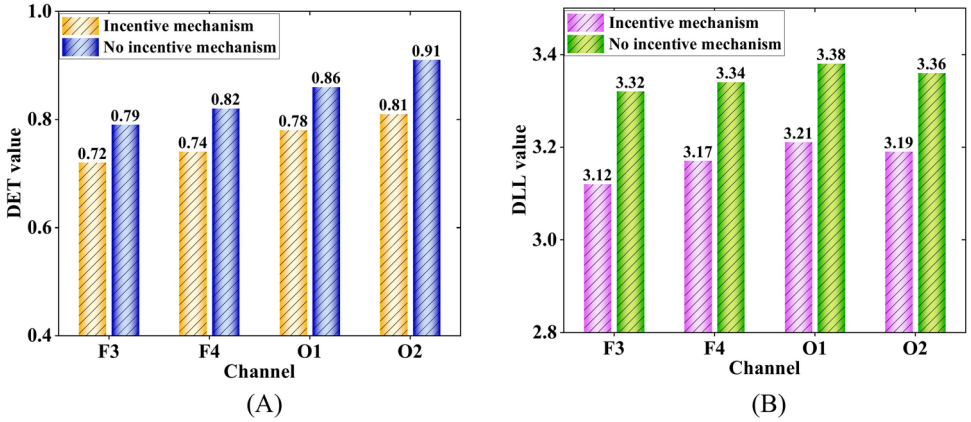

Fig. 11. Quantitative analysis results of EEG signals of subject A in two working states. (**A**) DET value; (**B**) DLL value.

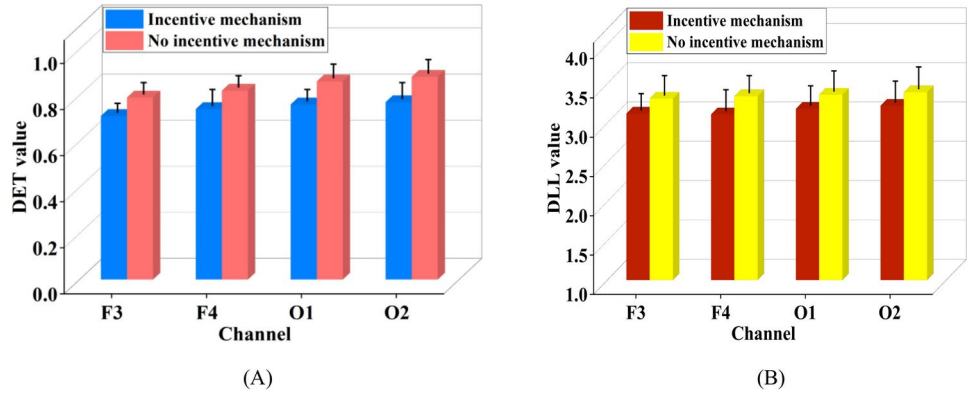

Fig. 12. Quantization analysis of EEG signals of 10 subjects in two working states. (**A**) DET value; (**B**) DLL value.

Methods	Accuracy/%	Precision/%	Recall/%	F1-score/%
RQA (DET)	97.64	97.29	96.96	97.14
RQA (DLL)	98.71	97.54	98.29	97.91
Phase space reconstruction and deep learning[45]	97.48	97.13	96.45	96.79
Modified cosine transform and LSTM-based masking[46]	96.98	96.78	96.12	96.45
Wavelet transform, reconstructed phase space, and deep learning networks[47]	96.67	96.56	96.32	96.44

Table 1. Comparison between RQA method and wavelet combined with machine learning method.

of phase space reconstruction and deep learning achieves an accuracy of 97.48%, precision of 97.13%, recall of 96.45%, and F1 score of 96.79%. The improved cosine transformation and LSTM-based method shows an accuracy of 96.98%, precision of 96.78%, recall of 96.12%, and F1 score of 96.45%. The method combining wavelet transform, reconstructed phase space, and deep learning network demonstrates an accuracy of 96.67%, precision of 96.56%, recall of 96.32%, and F1 score of 96.44%. Overall, the RQA methods outperform other deep learning methods across all metrics.

Al Fahoum et al. proposed a method to diagnose early schizophrenia by using PRS and continuous wavelet transform, which greatly enhanced the discrimination of EEG signals between normal individuals and patients with schizophrenia[48]. The results show that the proposed method performs well in terms of accuracy, precision, sensitivity, and robustness. In this study, the reconstructed phase space and continuous wavelet transform methods were used to classify the EEG signals under different excitation modes, and the classification results are shown in Fig. 13.

Figure 13 shows that the combination of PRS and continuous wavelet transform has achieved very desirable results in the classification task of EEG signals under different excitation modes. This method effectively

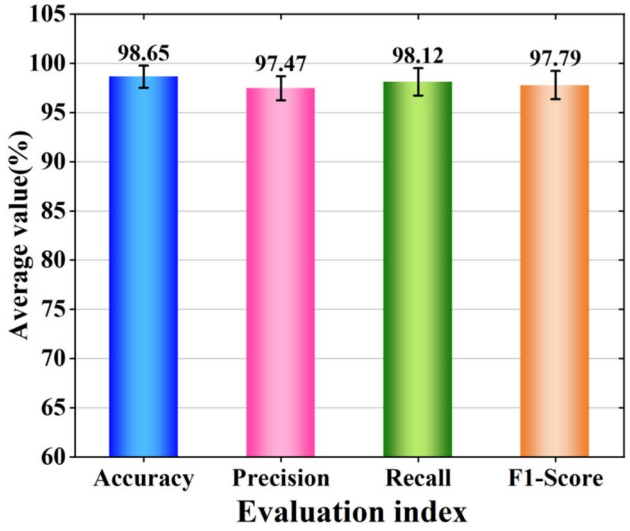

Fig. 13. Classification results obtained by combining the PRS with the continuous wavelet transform.

Methods	Accuracy (%)	Precision (%)	Recall (%)	F1-score (%)
RQA and decision tree	96.67	97.34	96.94	97.14
RQA and K-nearest neighbors[49]	97.87	98.23	96.89	97.56
RQA and adaptive boosting	98.22	97.66	98.13	97.89
RQA and CNN	98.41	98.34	97.39	97.86
RQA and RF	98.61	97.45	97.23	97.34

Table 2. Combination of RQA with other machine learning algorithms.

improves the feature extraction and pattern recognition ability of EEG signals, and shows excellent performance. Specifically, the precision is 98.65%, the precision is 97.47%, the recall is 98.12%, and the F1 score is 97.79%.

In this study, RQA was combined with other machine learning algorithms, such as decision tree and RF, to derive classification results, as shown in Table 2.

Table 2 shows the performance evaluation results of RQA combined with other machine learning algorithms. The evaluation metrics include accuracy, precision, recall, and F1 score. The combined algorithms are decision tree, KNN, adaptive boosting, CNN, and RF. From the results, the combination of RQA and different algorithms shows certain differences in various indicators, and the accuracy of RQA combined with RF is the highest, reaching 98.61%.

Work efficiency

The number of solder joints to be welded

In this study, the number of PCB solder joint soldering completed by 10 subjects in each working stage under the incentive mode without reward and punishment and the incentive mode with reward and punishment were counted, and the results are shown in Fig. 14.

Figure 14 shows that in the first stage, the number of completed piece-counts is zero because the subject has not yet started soldering the joints. As the subjects progress through the second, third, fourth, and fifth stages, the number of completed solder joints gradually increases. Comparative analysis reveals that the number of completed solder joints by participants with the reward and punishment incentive mechanism is significantly higher than that of those without the incentive model. This indicates that the reward and punishment incentive model proposed in this study effectively enhances workers' efficiency.

Quality of soldered PCB

Virtual welding refers to the failure of the solder joint to establish a proper electrical and mechanical connection during the electronic welding process, typically due to insufficient welding temperature, too short a welding time, or an improper welding process. The procedure for calculating the false welding defect rate is as follows: First, the welded circuit board is inspected for defects, and the number of solder joints with false welding defects is recorded. Next, the total number of solder joints in the batch is counted. Finally, the number of defective solder joints is divided by the total number of solder joints, and the result is multiplied by 100 to obtain the defect rate (expressed as a percentage). The false welding defect rate represents the proportion of solder joints with false welding defects in a batch, which reflects the quality of the welding process. Therefore, in this study, the false

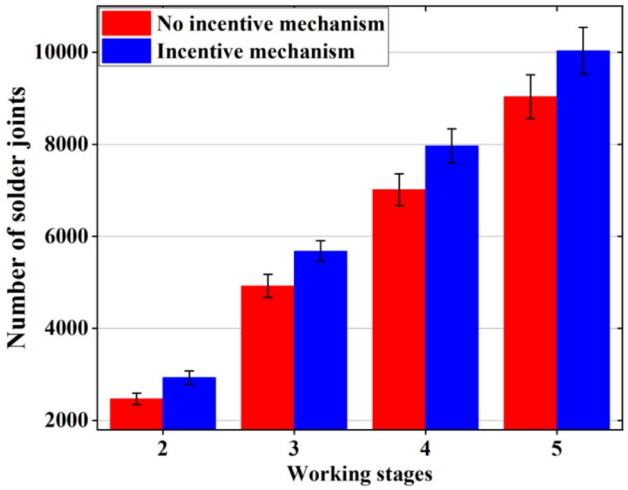

Fig. 14. The average value of the 10 subjects who completed the solder joint welding in different stages under the two working mechanisms.

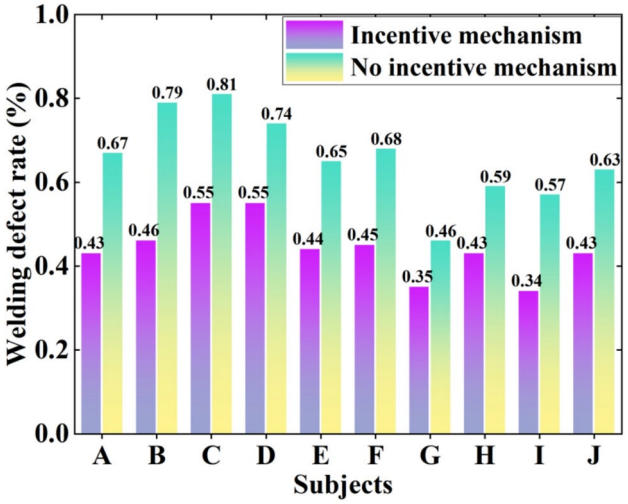

Fig. 15. Failure rate of welding under two working conditions.

welding defect rate is used as the standard to assess the quality of the soldered circuit board. The false welding defect rate for the subjects under the two working conditions is shown in Fig. 15.

As shown in Fig. 15, under the incentive mechanism of rewards and punishments, the weld defect rate of the subjects is generally lower than that of those without such an incentive mechanism. A t-test was conducted on the data in Fig. 15, and the results showed that the p-value for the two groups was 0.00038, which is less than 0.05, indicating a significant difference between the two groups. This suggests that the reward and punishment incentive mechanism effectively reduces the weld defect rate among circuit board workers. By implementing appropriate incentive and punishment measures, employees tend to pay more attention to their work details, thereby improving quality. Incentives motivate workers to strive for higher standards, particularly in identifying and avoiding weld defects, while penalties create pressure to reduce substandard welds.

Discussion

Novel methods for evaluating work efficiency

Al Fahoum et al. proposed a classification method combining PRS technology with deep neural networks (DNN) and attractor distribution features, which were applied to EEG signal analysis for depression and arrhythmia classification, respectively[50,51]. Through accurate pattern extraction and efficient classification, they achieved good experimental results in their respective fields, with high classification accuracy and low computational complexity. In contrast, this study proposes an innovative RQA-based method, which is combined with EEG signal analysis to explore the effects of reward and punishment incentive mechanisms on employee productivity. By comparing the chaotic characteristics of EEG signals under different excitation conditions, the RQA method not only quantifies changes in working efficiency but also effectively distinguishes between different working

states, achieving high classification accuracy with TWSVM. The innovation of this method lies in its integration of RQA with business management practices. From the perspective of human physiological characteristics, it provides a new and objective assessment tool with strong application prospects and operability. While PRS and DNN show outstanding performance, this study demonstrates unique innovation in its cross-domain application, combining psychology and physiology.

Compared to HRV and SCR, EEG offers significant advantages in assessing employee work efficiency. EEG can monitor brain activity in real time, providing high temporal resolution data that accurately reflect employees' attention, cognitive load, and emotional states, which facilitates an in-depth analysis of the neural basis of work efficiency[52]. While HRV primarily reflects autonomic nervous system function and can indirectly indicate stress and fatigue, it lacks immediate feedback on specific cognitive tasks and is heavily influenced by external factors[53]. SCR is mainly associated with emotional and stress responses. Although it can reflect changes in work stress, it does not directly reveal cognitive processes or task completion efficiency, and it exhibits significant individual differences[54]. Therefore, EEG provides more precise and comprehensive neural-level data for assessing work efficiency, making it superior to HRV and SCR. In this study, EEG signals were used to measure employee work efficiency under an incentive mechanism involving rewards and punishments. By integrating brain science, neuropsychology, and artificial intelligence technology, this approach offers a more accurate and objective method of evaluating work efficiency. It supports efficiency measurement from both physiological and psychological perspectives. Traditional work efficiency measures typically rely on employee performance data (such as task completion and working hours), which are easily influenced by external factors and personal biases. The EEG-based measurement method directly reflects the brain activity of employees, including psychological factors such as cognitive load, attention, concentration, and emotional fluctuations. By real-time monitoring of brain wave activity, employees' working status can be assessed more objectively, avoiding reliance on subjective evaluations or external behavioral performance[55]. Additionally, EEG signals are influenced by various factors, including physiological differences and changes in psychological states. To minimize potential bias from such factors, we use personalized modeling, adjusting and optimizing the model based on each individual's characteristics (such as their physiological and psychological states). This study also compares the time required for different methods to assess work efficiency.

This study used traditional employee efficiency evaluation methods, such as questionnaire surveys, quantitative indicators (output per unit time, task completion rate), behavioral observation, self-evaluation, combined with other evaluations, etc., and recorded the time consumed by each method. Then, these traditional methods were compared with the method proposed in this study, and the detailed data are shown in Table 3.

It can be seen from Table 3 that traditional assessment methods typically rely on interviews, questionnaires, and surveys. These methods are not only time-consuming but also prone to employee response bias. Managers also need to spend considerable time analyzing various indicators, making the entire process cumbersome. In contrast, the method proposed in this study requires employees to wear EEG signal acquisition equipment, with signals transmitted directly to the system for processing and analysis. This process requires minimal human intervention, significantly reducing the time needed for traditional evaluations. Managers no longer need to spend extensive time conducting one-on-one meetings with employees or collecting data through complex questionnaires and interviews.

Additionally, we have discussed the application of EEG monitoring in industrial environments. EEG signals provide valuable insights into brain activity but are highly susceptible to environmental noise, especially in noisy settings like industrial production workshops. To address this issue, advanced noise removal techniques are often necessary. Common noise removal methods include:

(1) Filtering techniques: High-pass, low-pass, or band-pass filters are used to eliminate noise within specific frequency ranges. For instance, power supply noise at 50/60 Hz can be removed, or motion artifacts at higher frequencies can be filtered out.
(2) ICA: This technique separates interfering components from EEG signals, removing elements unrelated to brain electrical activity, such as eye movements and electromyographic noise.
(3) Adaptive filtering: Adaptive filtering dynamically adjusts filter parameters based on real-time noise characteristics, making it adaptable to different noise types.
(4) Deep learning and machine learning methods: Recent advancements in signal processing, particularly deep learning-based methods, have made significant progress. Neural networks can be employed for automatic noise removal and to extract meaningful information from complex EEG data.

RQA method

To verify the stability of the RQA method used in this study for extracting EEG signal features, it is compared with four commonly used methods: sample entropy (SampEn)[56], Lempel–Ziv (LZ) complexity[57], power spectral density (PSD)[58], and fractal dimension[59]. These methods are used to extract the EEG signal characteristics of employees under the incentive mechanism of reward and punishment, and the dispersion coefficients for different working stages are calculated. The dispersion coefficient measures the degree of variability or spread of a data set relative to its mean. A low dispersion coefficient indicates less volatility, more concentrated data,

Methods	Behavior observation	Self-evaluation and other evaluation	Questionnaire survey	Quantitative index	Based on EEG signals (This study)
Time spent /min	100	70	50	30	15

Table 3. Time taken by different methods to evaluate work efficiency.

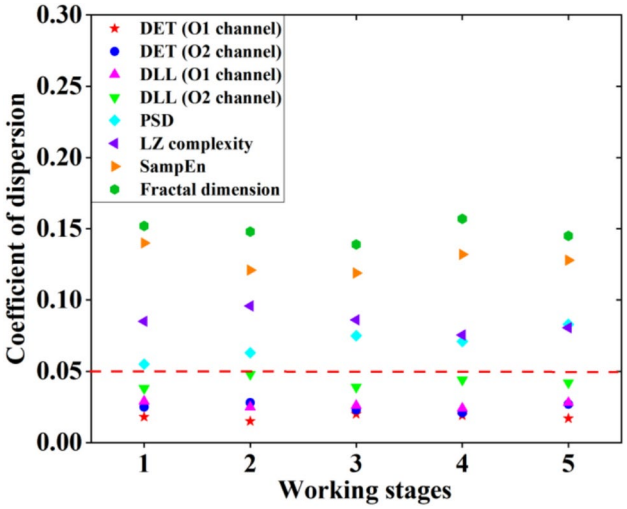

Fig. 16. Dispersion coefficients of different methods.

and lower variability. A high dispersion coefficient suggests greater volatility, data spread, and higher variability, typically implying a large difference between data points and higher uncertainty[60]. Additionally, the O1 and O2 channels, located in the occipital region of the brain, are primarily responsible for visual processing. These channels are situated on either side of the occipital lobe, and the activity in this area is closely related to visual information processing, attention, and working memory. During visual tasks, the activity in the occipital lobe reflects the efficiency and workload of visual processing[61]. Therefore, the EEG signals from the O1 and O2 channels can reflect the efficiency of workers in processing visual information, which in turn can affect overall work performance. For this reason, the study compares the dispersion coefficients of these channels. The results are shown in Fig. 16.

It can be seen in Fig. 16 that in the RQA method proposed in this study, the dispersion coefficients of the two feature parameters (DET and DLL) are lower than 0.05, which is lower than those of other methods, indicating that the RQA method exhibits lower data volatility and higher stability when extracting EEG signal features. The higher stability of the RQA method in extracting EEG signal features is attributed to its stronger robustness to noise and spurious periodicity. EEG signals often contain varying degrees of noise and pseudo-periodicity components. RQA can extract biologically meaningful signal features from complex dynamics by recursively analyzing system states, thus avoiding interference from noise and pseudo-periodicity. In contrast, traditional methods (such as PSD and SampEn) are more sensitive to noise and spurious periodicity, which can easily affect their stability and accuracy[62].

Application extension of the results

The application of this research extends across several fields. First, by regularly monitoring employees' EEG signals, companies can detect potential mental health issues early, especially in high-stress environments, and intervene promptly to prevent burnout and safety hazards. Second, intelligent EEG signal analysis allows companies to more accurately assess employees' work status and efficiency, dynamically optimize production processes, and improve overall productivity. In addition, real-time monitoring of EEG signals can enhance safety in high-risk jobs such as welding by preventing accidents caused by poor concentration or excessive psychological stress. In education and training, EEG technology can optimize learning outcomes by adjusting teaching content and methods based on the learner's state, thus improving efficiency. Finally, personalized task allocation based on EEG monitoring helps companies assign tasks according to employees' actual status and abilities, preventing overload and improving work efficiency. Overall, this approach not only enhances employee well-being but also boosts enterprise productivity and operations.

Limitations and future prospects

EEG signal acquisition faces multiple challenges. First, EEG signals are relatively weak and can be easily affected by artifacts, noise, and muscle electrical interference, leading to signal distortion and affecting the accuracy of brain activity measurements. With advancements in sensor technology, future EEG devices will become more sensitive and precise, capable of effectively eliminating interference and providing clearer signals. Additionally, by combining deep learning and artificial intelligence technologies, the accuracy of brain activity recognition in signal analysis can be improved. However, the high cost of EEG acquisition equipment may limit large-scale applications. Nevertheless, as technology advances, the prices of such equipment are gradually decreasing. Portable single-electrode EEG devices offer advantages in terms of cost and ease of use. In experiments involving human participants, research ethics must be strictly observed. Researchers should follow ethical guidelines, ensuring informed consent, data anonymity, and privacy protection.

Future work can focus on several aspects. First, integrating various physiological signals, such as heart rate and skin electrical response, can improve model accuracy and adaptability, creating a more comprehensive

physiological map to support decision-making. Second, developing a real-time adaptive incentive system based on monitoring employees' physiological and psychological states can optimize the work environment and task load to enhance work efficiency and employee well-being. For example, adjusting parameters like temperature, humidity, and lighting in real time; when employees are fatigued or under stress, automatically reducing task complexity or offering more rest time to prevent health issues. Finally, EEG technology has vast cross-industry application potential, providing insights into attention, emotional fluctuations, and fatigue levels. Personalized systems can adjust task difficulty based on employees' brainwave activities, optimizing task allocation, improving efficiency, and reducing health risks. Through these measures, EEG technology will play an essential role in enhancing productivity and protecting employee health.

Conclusions

This study aimed to evaluate the work efficiency of welding workers under an incentive mechanism of reward and punishment using EEG signal analysis, and proposed a new evaluation method based on the RQA method. The results indicate significant differences in the size, arrangement, and texture of blue and white squares in the ORP diagram of welding workers under different working conditions. Under the reward and punishment mechanism, the blue and white squares in the ORP diagram are smaller and more disordered. In contrast, without the reward or punishment mechanism, the squares are larger and more orderly. The RQA analysis shows that the two key characteristic parameters, DET and DLL values, are lower under the reward and punishment mechanism than under the mechanism without rewards or punishment. Additionally, the classification accuracy of EEG signals in the two working states reaches 98.71% using the SVM classification method. Compared to traditional work efficiency evaluation methods, this approach significantly reduces the evaluation time, taking only 15 min. Furthermore, compared with traditional signal feature extraction methods, the RQA method shows better stability and robustness. Based on the results, the feasibility of integrating this method with wearable EEG devices or real-time monitoring systems should be further explored. By combining it with a real-time monitoring system, it would allow continuous tracking and immediate feedback of the reward and punishment incentive mechanism's effect on welding workers, providing a more efficient and accurate incentive management strategy for enterprises. In addition, EEG-based reward and punishment recommendations could not only optimize existing work efficiency evaluation methods but also offer a scientific basis for customized incentive strategies. Therefore, future research will expand the scope of application of this method and explore its applicability in different industries to enhance its practical value.

Data availability

The datasets generated and/or analysed during the currentstudy are not publicly availabledue [REASON WHY DATA ARENOT PUBLIC] but are availablefrom the corresponding authoron reasonable request. The effective data email: zhangqian2119909@163.com.

Received: 21 November 2024; Accepted: 31 March 2025
Published online: 05 April 2025

References

1. Pane, I. M. B. T. et al. The effect of the implementation of reward, incentive, and punishment methods on employee performance at PT Anugerah Alam Berastagi. *J. Res. Bus. Econ. Educ.* **5**(3), 90–98 (2023).
2. Oleghe, O. & Salonitis, K. Improving the efficacy of the lean index through the quantification of qualitative lean metrics. *Procedia Cirp* **37**, 42–47 (2015).
3. Zhou, J. & He, W. Efficiency-oriented training and development based on service process observation and assessment in the workplace. *Int. J. Product. Perform. Manag.* **73**(6), 1909–1925 (2024).
4. Voronkova, O. V. et al. Assessment of the influence of human factor on the working process effectiveness as a factor for improving the efficiency of production management at industrial enterprises. *Rev. Espacios* **39**, 48 (2018).
5. Li, M. et al. The impact of physiological and psychological fatigue on work efficiency: A case study of parcel sorting work. *Sensors* **24**(18), 5989 (2024).
6. Kc, D. S. et al. Task selection and workload: A focus on completing easy tasks hurts performance. *Manage. Sci.* **66**(10), 4397–4416 (2020).
7. Rao, A. S. et al. Real-time monitoring of construction sites: Sensors, methods, and applications. *Autom. Constr.* **136**, 104099 (2022).
8. Fauquet-Alekhine, P., Rouillac, L. & Granry, J. C. Subjective versus objective assessment of short term occupational stress: Bias and analysis of self-assessment of high stress levels. *J. Adv. Med. Med. Res.* **32**(10), 50–64 (2020).
9. Bornstein, R. F. Evidence-based psychological assessment. *J. Pers. Assess.* **99**(4), 435–445 (2017).
10. Hasnaoui, L. H. & Djebbari, A. Leveraging epilepsy detection accuracy through burst energy integration in CWT and decision tree classification of EEG signals. *Biomed. Eng. Appl. Basis Commun.* **2024**, 2450052 (2024).
11. Hasnaoui, L. H. & Djebbari, A. Robust dimensionality-reduced epilepsy detection system using EEG wavelet packets and machine learning. *Res. Biomed. Eng.* **1**, 1–22 (2024).
12. Hasnaoui, L. H., Benabdallah, A. & Djebbari, A. Investment of biomedical applications in marketing: Electroencephalogram-based consumer decision prediction. *Biomed. Eng. Appl. Basis Commun.* **35**(04), 2350013 (2023).
13. Christie, G. J. & Tata, M. S. Right frontal cortex generates reward-related theta-band oscillatory activity. *Neuroimage* **48**(2), 415–422 (2009).
14. Olszewska-Guizzo, A. et al. Features of urban green spaces associated with positive emotions, mindfulness and relaxation. *Sci. Rep.* **12**(1), 20695 (2022).
15. Pizzagalli, D. A. et al. Reward and punishment processing in the human brain: Clues from affective neuroscience and implications for depression research Neuroscience of decision making. *Psychol. Press* **1**, 199–220 (2011).
16. Lee, J., Kim, C. & Lee, K. C. An empirical approach to analyzing the effects of stress on individual creativity in business problem-solving: emphasis on the electrocardiogram, electroencephalogram methodology. *Front. Psychol.* **13**, 705442 (2022).
17. Nayana, B. R. & Geethanjali, P. Analysis of statistical time-domain features effectiveness in identification of bearing faults from vibration signal. *IEEE Sens. J.* **17**(17), 5618–5625 (2017).

18. Chikhi, S., Matton, N. & Blanchet, S. EEG power spectral measures of cognitive workload: A meta-analysis. *Psychophysiology* **59**(6), e14009 (2022).
19. Ha, L. D. et al. Time-resolved electrochemical impedance spectroscopy of stochastic nanoparticle collision: Short time Fourier transform versus continuous wavelet transform. *Small* **19**(33), 2302158 (2023).
20. Datseris, G. et al. Estimating fractal dimensions: A comparative review and open source implementations. *Chaos Interdiscipl. J. Nonlinear Sci.* **33**, 10 (2023).
21. Chakladar, D. D. et al. Cognitive workload estimation using variational autoencoder and attention-based deep model. *IEEE Trans. Cogn. Dev. Syst.* **15**(2), 581–590 (2022).
22. Yoo, G., Kim, H. & Hong, S. Prediction of cognitive load from electroencephalography signals using long short-term memory network. *Bioengineering* **10**(3), 361 (2023).
23. Xiong, R. et al. Pattern recognition of cognitive load using EEG and ECG signals. *Sensors* **20**(18), 5122 (2020).
24. Vanneste, P. et al. Towards measuring cognitive load through multimodal physiological data. *Cogn. Technol. Work* **23**, 567–585 (2021).
25. Gutiérrez, Á. et al. Biosignals monitoring of first responders for cognitive load estimation in real-time operation. *Appl. Sci.* **13**(13), 7368 (2023).
26. Mora-Sánchez, A. et al. A brain–computer interface for the continuous, real-time monitoring of working memory load in real-world environments. *Cogn. Neurodyn.* **14**, 301–321 (2020).
27. Webber, C. L. Jr. & Zbilut, J. P. Recurrence quantification analysis of nonlinear dynamical systems. *Tutor. Contemp. Nonlinear Methods Behav. Sci.* **2005**(94), 26–94 (2005).
28. Zhang, Z., Song, F. & Song, Z. Promoting knowledge sharing in the workplace: Punishment v reward. *Chaos Solitons Fract.* **131**, 109518 (2020).
29. Rojas, M., Méndez, A. & Watkins-Fassler, K. The hierarchy of needs empirical examination of Maslow's theory and lessons for development. *World Dev.* **165**, 106185 (2023).
30. LaLumiere, R. T. & Kalivas, P. W. Motivational systems: Rewards and incentive value. *Handb. Psychol. Behav. Neurosci.* **2**, 395–421 (2013).
31. Jose, R. J. S. et al. Enhancing staff's work motivation in Vietnamese companies. *Turk. J. Comput. Math. Educ. (TURCOMAT)* **12**(14), 4402–4410 (2021).
32. Wang, X. et al. Stability of the evolutionary game system and control strategies of behavior instability in coal mine safety management. *Complexity* **2019**(1), 6987427 (2019).
33. Schinkel, S., Marwan, N. & Kurths, J. Order patterns recurrence plots in the analysis of ERP data. *Cogn. Neurodyn.* **1**, 317–325 (2007).
34. Katsavrias, C. et al. Application of wavelet methods in the investigation of geospace disturbances: A review and an evaluation of the approach for quantifying wavelet power. *Atmosphere* **13**(3), 499 (2022).
35. Huo, Z. et al. Entropy measures in machine fault diagnosis: Insights and applications. *IEEE Trans. Instrum. Meas.* **69**(6), 2607–2620 (2020).
36. Benmebarek, S. & Chettih, M. Chaotic analysis of daily runoff time series using dynamic, metric, and topological approaches. *Acta Geophys.* **72**(4), 2633–2651 (2024).
37. Noakes, L. The Takens embedding theorem. *Int. J. Bifurc. Chaos* **1**(04), 867–872 (1991).
38. Rhodes, C. & Morari, M. The false nearest neighbors algorithm: An overview. *Comput. Chem. Eng.* **21**, S1149–S1154 (1997).
39. Ji, C. et al. Real-time industrial process fault diagnosis based on time delayed mutual information analysis. *Processes* **9**(6), 1027 (2021).
40. Liu, J. et al. A new EEG determinism analysis method based on multiscale dispersion recurrence plot. *Biomed. Signal Process. Control* **80**, 104301 (2023).
41. Al Fahoum, A., Al Omari, A. & Al Omari, G. Development of a novel light-sensitive PPG model using PPG scalograms and PPG-NET learning for non-invasive hypertension monitoring. *Heliyon* **10**(21), 39745 (2024).
42. Jimenez-Castaño, C. et al. Kreĭn twin support vector machines for imbalanced data classification. *Pattern Recogn. Lett.* **182**, 39–45 (2024).
43. Hung, T. M. et al. Visuomotor expertise and dimensional complexity of cerebral cortical activity. *Med. Sci. Sports Exerc.* **40**(4), 752–759 (2008).
44. Jung, J. Y., Cho, H. Y. & Kang, C. K. Brain activity during a working memory task in different postures: An EEG study. *Ergonomics* **63**(11), 1359–1370 (2020).
45. Al, F. A. Early detection of neurological abnormalities using a combined phase space reconstruction and deep learning approach. *Intell. Based Med.* **8**, 100123 (2023).
46. Al-Zaben, A. et al. Improved recovery of cardiac auscultation sounds using modified cosine transform and LSTM-based masking. *Med. Biol. Eng. Comput.* **62**(8), 2485–2497 (2024).
47. Al Fahoum, A. & Zyout, A. Wavelet transform, reconstructed phase space, and deep learning neural networks for EEG-based schizophrenia detection. *Int. J. Neural Syst.* **34**(9), 2450046–2450046 (2024).
48. Al, F. A. Enhanced cardiac arrhythmia detection utilizing deep learning architectures and multi-scale ECG analysis. *Tuijin Jishu/J. Propul. Technol.* **44**(6), 5539–5554 (2023).
49. Sun, J. et al. An effective method of weld defect detection and classification based on machine vision. *IEEE Trans. Ind. Inf.* **15**(12), 6322–6333 (2019).
50. Al-Fahoum, A. S. & Reza, A. M. Perceptually tuned JPEG coder for echocardiac image compression. *IEEE Trans. Inf. Technol. Biomed.* **8**(3), 313–320 (2004).
51. Al Fahoum, A. S. & Qasaimeh, A. M. A practical reconstructed phase space approach for ECG arrhythmias classification. *J. Med. Eng. Technol.* **37**(7), 401–408 (2013).
52. Zanetti, R. et al. Real-time EEG-based cognitive workload monitoring on wearable devices. *IEEE Trans. Biomed. Eng.* **69**(1), 265–277 (2021).
53. Hao, T. et al. Linear and nonlinear analyses of heart rate variability signals under mental load. *Biomed. Signal Process. Control* **77**, 103758 (2022).
54. García-Moreno, J. A. et al. Cognitive reserve and anxiety interactions play a fundamental role in the response to the stress. *Front. Psychol.* **12**, 673596 (2021).
55. Lu, M. et al. Research on work efficiency and light comfort based on EEG evaluation method. *Build. Environ.* **183**, 107122 (2020).
56. Ru, Y. et al. Epilepsy detection based on variational mode decomposition and improved sample entropy. *Comput. Intell. Neurosci.* **2022**(1), 6180441 (2022).
57. Hu, J., Gao, J. & Principe, J. C. Analysis of biomedical signals by the Lempel-Ziv complexity: the effect of finite data size. *IEEE Trans. Biomed. Eng.* **53**(12), 2606–2609 (2006).
58. Malan, N. S. et al. Functional connectivity and power spectral density analysis of EEG signals in trained practitioners of Bhramari pranayama. *Biomed. Signal Process. Control* **84**, 105003 (2023).
59. Ruiz-Padial, E. & Ibáñez-Molina, A. J. Fractal dimension of EEG signals and heart dynamics in discrete emotional states. *Biol. Psychol.* **137**, 42–48 (2018).
60. Eappen, C. V., Sedory, S. A. & Singh, S. Ratio and regression type estimators of a new measure of coefficient of dispersion. *Commun. Stat. Simul. Comput.* **51**(4), 1899–1920 (2022).

61. Ma, C. et al. Applying gestalt similarity to improve visual perception of interface color quantity: An EEG study. *Int. J. Ind. Ergon.* **100**, 103521 (2024).
62. Haake, L. et al. Global temporal typing patterns in foreign language writing: Exploring language proficiency through recurrence quantification analysis (RQA). *Read. Writ.* **37**(2), 385–417 (2024).

Acknowledgements
This work was supported by the Northeast Electric Power University [BSJXM-201521]; Jilin City Science and Technology Bureau [20166012].

Author contributions
Zhang Qian and Fuwang Wang conceived and designed the experiments; Mingyue Guo analyzed the data; Fuwang Wang contributed reagents/materials/analysis tools; Zhang Qian and Mingyue Guo wrote the main manuscript text. All authors reviewed the manuscript.

Declarations

Competing interests
The authors declare no competing interests.

Ethical approval
All subjects were informed of the purpose of the study and all consented in writing to be included in the study. The Ethical Committee of Northeast Electric Power University Hospital approved the research protocol in accordance with the ethical guidelines of the World Medical Association (Declaration of Helsinki).

Additional information
Correspondence and requests for materials should be addressed to Z.Q.

Reprints and permissions information is available at www.nature.com/reprints.

Publisher's note Springer Nature remains neutral with regard to jurisdictional claims in published maps and institutional affiliations.